Regioselectivity of acid-catalyzed cyclization of 1-(3,4-dialkylaryl)-3-chloropropan-1-ones to indanones. Comparison of experimental data and results of computer simulation

P. V. Ivchenko, I. E. Nifant´ev, L. Yu. Ustynyuk, and V. A. Ezerskii*

Department of Chemistry, M. V. Lomonosov Moscow State University, 1 Leninskie Gory, 119992 Moscow, Russian Federation. Fax: +7 (495) 939 4523. E-mail: inpv@org.chem.msu.ru

The acid-catalyzed cyclization of 1-(3,4-dialkylaryl)-3-chloropropan-1-ones to dialkylindanones *via* the intermediate formation of (3,4-dialkylaryl)propenones was studied. This reaction affords isomeric products: 5,6-dialkylindan-1-ones and 4,5-dialkylindan-1-ones. The DFT quantum chemical calculation results correlate with the experimental data and suggest that the structural factors affect the ratio of products.

Key words: indanones, Friedel—Crafts acylation, Nazarov reaction, quantum chemical calculations.

Substituted indanones[1] are widely used in organic synthesis and organometallic chemistry. Among many methods for their synthesis, one of the most attractive is the acylation of aromatic hydrocarbons with unsaturated acid chlorides in the presence of electrophilic catalysts followed by the cyclization of intermediate aryl vinyl ketones to indanones (Scheme 1).[2,3] This method is experimentally simple and the starting reactants are accessible. Along with unsaturated acid derivatives, 2- or 3-alkanoyl chlorides can be used.[4,5] In the case of 3-halogencarboxylic acids, the reaction is sometimes carried out in two steps, and in the second step 2-haloalkyl aryl ketone is subjected to the acid-catalyzed cyclization (Scheme 1). The reaction also proceeds through the intermediate formation of the protonated form of aryl vinyl ketone.[6]

The key step of the processes discussed is the Nazarov reaction, *viz.*, the acid-catalyzed cyclization of aryl vinyl ketones to indanones.[6] In the case of substrates substituted to the benzene ring, the reaction affords mixtures of isomeric indanones. In this case, hydrocarbons formally similar in structure and electronic properties sometimes give different products. For example, tetralin is predominantly transformed into the α-cyclization product, whereas indane mainly yields the β-product[3] (Scheme 2). Reasons for the observed difference in reactivity are unclear and cannot be explained by general concepts with allowance for only the *ortho*/*para*-orienting effects of alkyl substituents.

We attempted to find reasons for these differences in reactivity. For this purpose we studied the acid-catalyzed cyclization of the series of 1-(3,4-dialkylaryl)-3-chloropropan-1-ones **1**—**4**. To interpret the data obtained, we studied this process by the DFT method and theoretically estimated the ratio of α- and β-isomers. Since the results of calculations qualitatively coincided with the experimental data, we proposed the factors determining the regioselectivity of this reaction.

Scheme 1

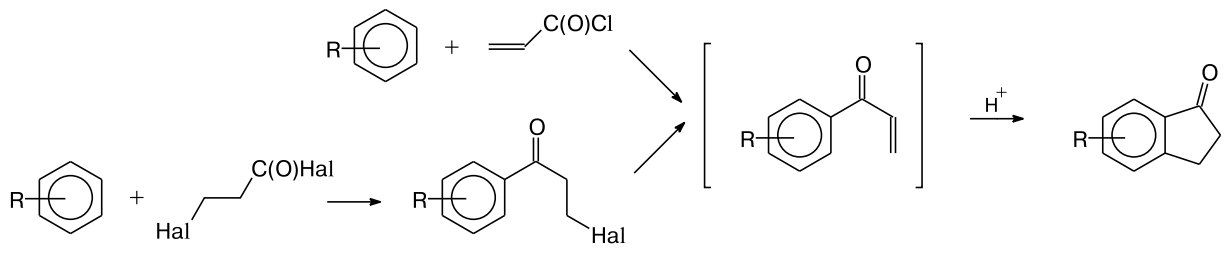

Published in Russian in *Izvestiya Akademii Nauk. Seriya Khimicheskaya,* No. 5, pp. 909—915, May, 2009.

Scheme 2

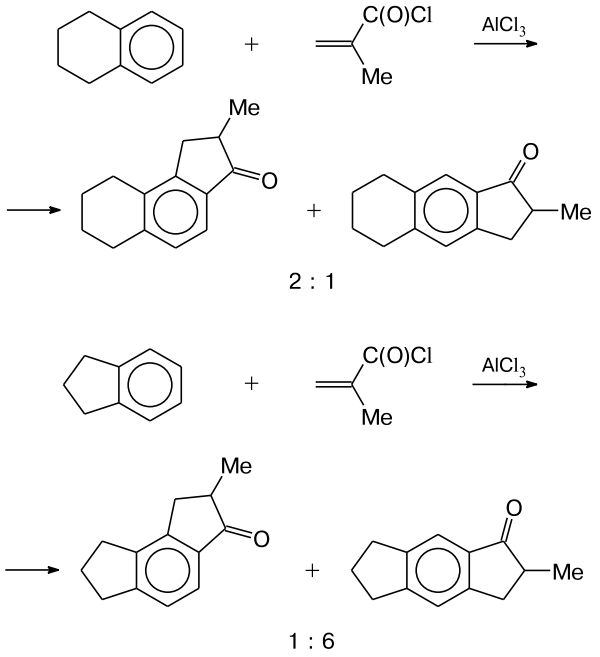

Results and Discussion

1-(3,4-Dialkylaryl)-3-chloropropan-1-ones **1—4** have earlier been synthesized by the reaction of the corresponding arenes with 3-chloropropionyl chloride in the presence of $AlCl_3$ (Scheme 3).[7,8] For compounds **1—3** we used CH_2Cl_2 as a solvent. An attempt to obtain compound **4** in this solvent resulted in resinification; the product was synthesized in 63% yield when the reaction was carried out in nitromethane. The yields of the products (except for compound **4**) were high. The moderate yield of compound **4** is due, most likely, to side electrophilic reactions accompanied by strained four-membered ring opening. It should be mentioned that the acylation proceeds selectivity to position 4 in all cases.

The cyclization of ketones **1—4** to indanones was carried out on heating in sulfuric acid. The ratios of the reaction products listed in Table 1 were calculated from the NMR spectra of the crude materials. The reaction rate decreasing in the series of compounds **4** > **3** > **1** > **2** was approximately evaluated. Compound **2** is least reactive, although in the series of fused aliphatic rings the six-membered fused fragment is most electron-donating.[9]

Table 1. Yields and ratios of cyclization products of ketones **1—4** to indanones **5—12**

Compound	RR	Yield (%)	Ratio	
1	Me, Me	98	**5** : **6**	1 : 2
2	$(CH_2)_4$	98	**7** : **8**	1 : 0.7
3	$(CH_2)_3$	94	**9** : **10**	1 : 4.5
4	$(CH_2)_2$	63	**11** : **12**	1 : 13

The obtained experimental data were further verified using computer simulation.

The reaction affording isomeric dialkylindan-1-ones occurs *via* the mechanism shown in Scheme 4.[6] In the first step, aryl vinyl ketones **13—16** and the corresponding protonated forms **17—20** are formed upon the action of H_2SO_4 on 1-aryl-3-chloropropan-1-ones. Compounds **17—20** undergo cyclization *via* the Nazarov mechanism to form cationic intermediates **21**$^{\neq}$**—28**$^{\neq}$, which then eliminate a proton to produce enolic forms **29—36**. Their isomerization affords indanones **5—12**.

The key step of the reaction is the cyclization of aryl vinyl ketones **17—20** protonated at oxygen (Scheme 4), which can exist as different conformers. The conformers involved in the Nazarov reaction are shown in Scheme 4. The cyclization of **α-17—α-20** affords indanones **5**, **7**, **9**, and **11**, respectively; compounds **β-17—β-20** are cyclized to form isomeric indanones **6**, **8**, **10**, and **12**, respectively.

The ratio of the reaction products is determined by the step of cyclization of protonated vinyl ketones **17—20**. The structures and energies of intermediates **17—20** and transitions states **21**$^{\neq}$**—28**$^{\neq}$ were calculated. The unique PRIRODA program was used for the calculations.[10] The calculations were performed for the gas phase. This simplification of the calculation procedure is acceptable, because the task is the qualitative estimation of the relative energies and the search for structural factors deter-

Scheme 3

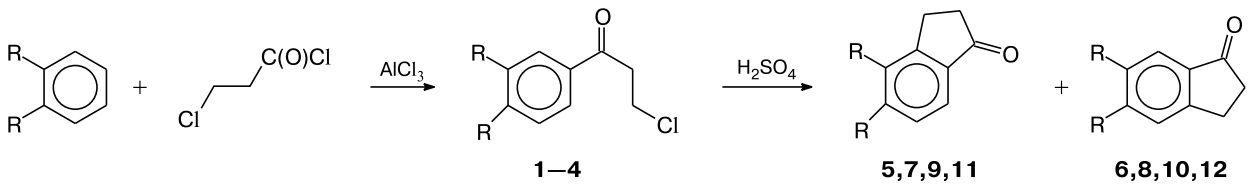

R = Me (**1**, **5**, **6**)
R, R = $(CH_2)_4$ (**2**, **7**, **8**), $(CH_2)_3$ (**3**, **9**, **10**), $(CH_2)_2$ (**4**, **11**, **12**)

Scheme 4

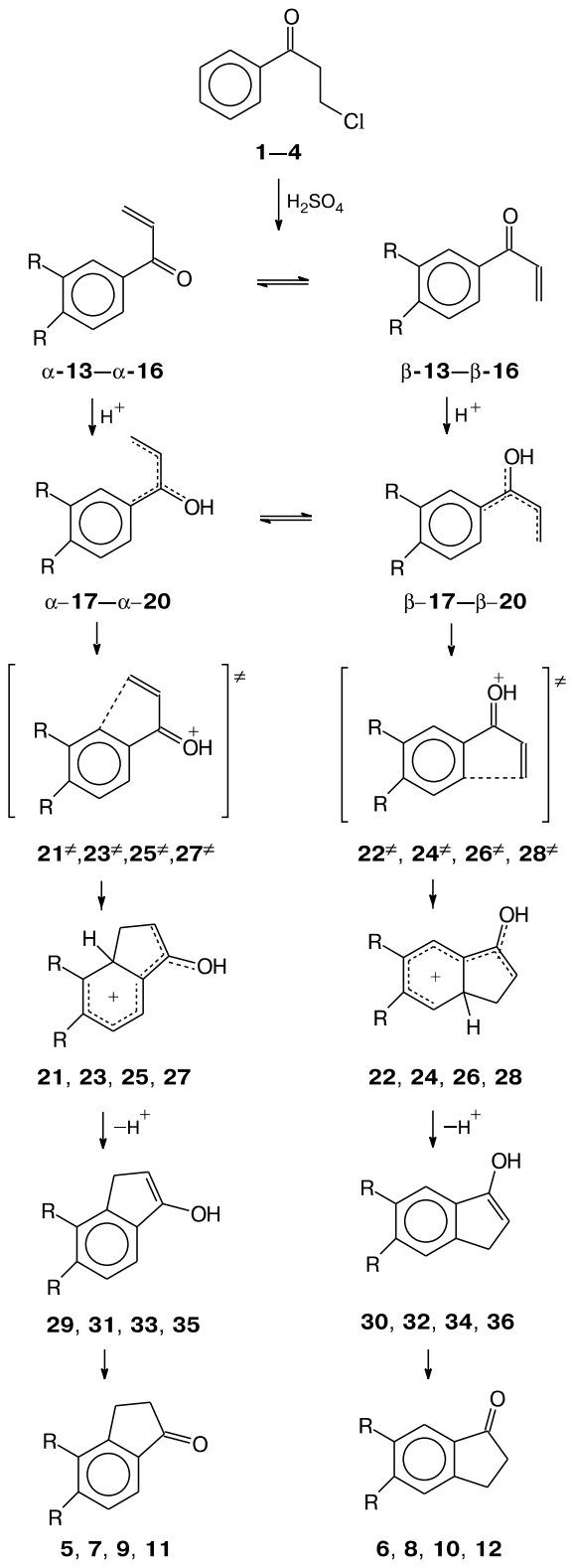

R = Me (**5**, **6**, **13α,β**, **17α,β**, **21**≠, **22**≠, **21**, **22**, **29**, **30**)
R, R = $(CH_2)_4$ (**7**, **8**, **14α,β**, **18α,β**, **23**≠, **24**≠, **23**, **24**, **31**, **32**)
R, R = $(CH_2)_3$ (**9**, **10**, **15α,β**, **19α,β**, **25**≠, **26**≠, **25**, **26**, **33**, **34**)
R, R = $(CH_2)_2$ (**11**, **12**, **16α,β**, **20α,β**, **27**≠, **28**≠, **27**, **28**, **35**, **36**)

mining the regioselectivity in the series of the same-type compounds.

The free energies that allow one to determine the activation energies were calculated for ketones **17**—**20** and transition states **21**≠—**28**≠. The results obtained are given in Table 2 and as a diagram in Fig. 1. The data presented show that β-cyclization is more favorable for intermediates **17**, **19**, and **20**, whereas for compound **18** α- and β-cyclizations are almost equiprobable.

The activation energy values for the competitive processes make it possible to calculate the ratios of α- and β-cyclization products and compare the data obtained with the experimental results (Table 3). It is seen that the theoretical and experimental data are rather close. In addition, the calculated energy values correlate with the experimentally observed cyclization rates of aryl vinyl ketones **13**—**16**.

Table 2. Activation energies of the competitive processes for indanones **5**—**12** at 360 K

Compound	Isomer	ΔG_{act}/kcal mol^{-1}
5	α	20.18
7	α	19.55
9	α	20.19
11	α	20.04
6	β	19.53
8	β	19.55
10	β	19.09
12	β	18.48

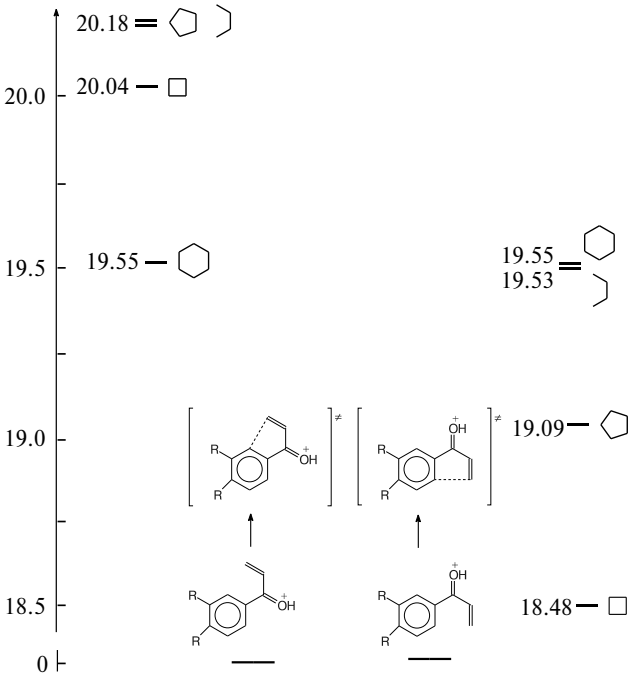

Fig. 1. Calculated activation energies of the competitive reactions of cyclization of vinyl ketones **17**—**20** at 360 K.

Table 3. Products and their ratio

Products α : β	Ratio	
	Experiment	Calculation
5 : **6**	1 : 2	1 : 2.5
7 : **8**	1 : 0.7	1 : 1
9 : **10**	1 : 4.5	1 : 4.6
11 : **12**	1 : 13	1 : 8.8

Both the experiment and calculation show that the fraction of the β-cyclization product increases with a decrease in the size of the fused cycle. In order to establish the factors determining the regioselectivity of formation of isomeric indanones, it is reasonable to analyze the geometry of the initial cationic intermediates and transition states leading to the formation of isomeric indanones (Schemes 5 and 6). Selected structural parameters of inermediates **α-17—α-20** → **21**$^{\neq}$, **23**$^{\neq}$, **25**$^{\neq}$, **27**$^{\neq}$ are given in Tables 4 and 5, and those for intermediates **β-17—β-20** → **22**$^{\neq}$, **24**$^{\neq}$, **26**$^{\neq}$, **28**$^{\neq}$ are presented in Tables 6 and 7.

Scheme 5

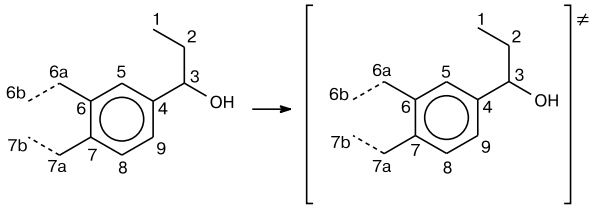

Scheme 6

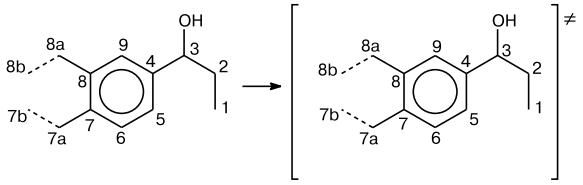

Still in the step of intermediates **17—20**, it is seen that the C(6)—C(7) (α) and C(7)—C(8) (β) bonds are shortened with a decrease in the fused cycle size, which elongates the C(4)—C(5) bond and facilitates the cyclization to occur.

Figure 2 shows the change in the bond lengths in the aromatic rings during ketone transformation **17—20** → → **21**$^{\neq}$—**28**$^{\neq}$. The key structural fragment determining the regioselectivity of cyclization is the distortion of the aromatic ring on going to the transition state: the regular elongation of the C(4)—C(5) and C(5)—C(6) bonds at the C(5) atom at which the electrophilic attack occurs is accompanied by the elongation of the C(7)—C(8) and C(8)—C(9) symmetric bonds, and the lengths of other bonds decrease. These distortions are of the same type: the C(4)—C(5) bond elongates by 0.024—0.029 Å, and the C(7)—C(8) symmetric bond elongates by 0.009—0.011 Å in the case of α-cyclization and by 0.012—0.014 Å for β-cyclization. The C(6)—C(7) bond becomes shorter by 0.016—0.018 Å (α-cyclization) and by 0.017—0.019 Å (β-cyclization).

Distortions of the benzene ring structure necessarily involve the alicyclic fragment fused with this ring, be-

Table 4. Selected bond lengths in intermediates **α-17—α-20** and in transition states **21**$^{\neq}$, **23**$^{\neq}$, **25**$^{\neq}$, and **27**$^{\neq}$

Bond	*d*/Å							
	α-17	**21**$^{\neq}$	**α-18**	**23**$^{\neq}$	**α-19**	**25**$^{\neq}$	**α-20**	**27**$^{\neq}$
	6a = 6b, 7a = 7b*				6b = 7b*		6a = 6b, 7a = 7b*	
4—5	1.423	1.449	1.421	1.448	1.427	1.456	1.434	1.463
5—6	1.389	1.429	1.391	1.430	1.382	1.422	1.377	1.416
6—7	1.425	1.407	1.420	1.402	1.416	1.399	1.410	1.394
7—8	1.413	1.422	1.416	1.425	1.405	1.414	1.398	1.409
8—9	1.380	1.393	1.377	1.390	1.384	1.396	1.390	1.400
4—9	1.421	1.401	1.424	1.404	1.426	1.405	1.432	1.411
6—6a	1.504	1.502	1.515	1.511	1.511	1.507	1.522	1.519
7—7a	1.495	1.504	1.503	1.513	1.499	1.510	1.512	1.520
6a—6b	—	—	1.532	1.535	1.548	1.553	—	—
7a—7b	—	—	1.531	1.534	1.548	1.552	—	—
6b—7b	—	—	1.530	1.533	—	—	1.580	1.583

* The positions are shown in Scheme 5. The coinciding positions are marked with the sign "=".

Table 5. Selected bond angles in intermediates **α-17**—**α-20** and in transition states **21**$^{\neq}$, **23**$^{\neq}$, **25**$^{\neq}$, and **27**$^{\neq}$

Angle	ω/deg							
	α-17	**21**$^{\neq}$	**α-18**	**23**$^{\neq}$	**α-19**	**25**$^{\neq}$	**α-20**	**27**$^{\neq}$
	6a = 6b, 7a = 7b				6b = 7b		6a = 6b, 7a = 7b	
4—5—6	121.54	120.59	121.63	120.63	119.25	118.28	115.91	114.91
5—6—7	118.75	118.30	118.71	118.15	120.15	119.58	122.20	121.40
6—7—8	119.56	119.49	119.61	119.68	121.08	121.11	122.98	100.40
7—8—9	121.68	123.15	121.73	123.09	119.33	120.75	116.03	117.37
8—9—4	119.32	118.29	119.24	118.20	120.28	119.20	121.70	120.56
9—4—5	119.12	119.77	119.06	119.73	119.90	120.68	121.16	122.08
7—6—6a	120.73	121.67	121.18	122.01	110.13	111.03	93.15	93.69
6—6a—6b	—	—	113.10	113.15	103.28	103.23	86.49	86.38
6a—6b—7b	—	—	110.08	110.15	104.86	105.15	—	—
6b—7b—7a	—	—	110.47	110.56	—	—	—	—
7b—7a—7	—	—	114.55	113.76	103.72	103.31	87.0	86.49
7a—7—6	120.51	120.78	121.37	121.54	110.20	110.38	93.28	93.43

Table 6. Selected bond lengths in intermediates **β-17**—**β-20** and in transition states **22**$^{\neq}$, **24**$^{\neq}$, **26**$^{\neq}$, and **28**$^{\neq}$

Bond	*d*/Å							
	β-17	**22**$^{\neq}$	**β-18**	**24**$^{\neq}$	**β-19**	**26**$^{\neq}$	**β-20**	**28**$^{\neq}$
	7a = 7b, 8a = 8b			7b = 8b			7a = 7b, 8a = 8b	
4—5	1.421	1.466	1.424	1.448	1.426	1.451	1.431	1.459
5—6	1.383	1.422	1.380	1.420	1.386	1.425	1.393	1.431
6—7	1.410	1.391	1.413	1.392	1.402	1.384	1.395	1.379
7—8	1.429	1.443	1.424	1.438	1.420	1.434	1.413	1.425
8—9	1.387	1.399	1.389	1.401	1.381	1.393	1.375	1.386
4—9	1.422	1.402	1.421	1.400	1.427	1.406	1.433	1.413
7—7a	1.494	1.502	1.503	1.515	1.499	1.509	1.513	1.522
8—8a	1.503	1.499	1.514	1.511	1.510	1.505	1.521	1.518
7a—7b	—	—	1.532	1.534	1.548	1.551	—	—
8a—8b	—	—	1.532	1.535	1.548	1.549	—	—
7b—8b	—	—	1.530	1.532	—	—	1.580	1.581

Table 7. Selected bond angles (ω) in intermediates **β-17**—**β-20** and in transition states **22**$^{\neq}$, **24**$^{\neq}$, **26**$^{\neq}$, and **28**$^{\neq}$

Angle	ω/deg							
	β-17	**22**$^{\neq}$	**β-18**	**24**$^{\neq}$	**β-19**	**26**$^{\neq}$	**β-20**	**28**$^{\neq}$
4—5—6	119.39	118.44	119.32	118.39	120.35	119.35	121.77	120.71
5—6—7	121.59	121.18	121.64	121.26	119.22	118.83	115.87	115.39
6—7—8	119.56	119.51	119.59	119.51	121.04	120.96	122.98	123.05
7—8—9	118.81	119.98	118.79	120.00	120.26	121.50	122.36	123.57
8—9—4	121.48	120.51	121.55	120.57	119.14	118.16	115.74	114.80
9—4—5	119.15	119.96	119.07	119.91	119.95	120.76	121.24	122.02
7—8—8a	120.65	120.07	121.09	120.88	110.02	109.77	93.10	93.01
8—8a—8b	—	—	113.21	114.22	103.39	103.78	86.58	87.13
8a—8b—7b	—	—	110.18	110.29	104.81	104.50	—	—
8b—7b—7a	—	—	110.43	110.02	—	—	—	—
7b—7a—7	—	—	114.39	113.66	103.76	103.36	87.11	86.98
7a—7—8	120.44	120.04	121.24	113.66	110.14	109.68	93.20	92.87

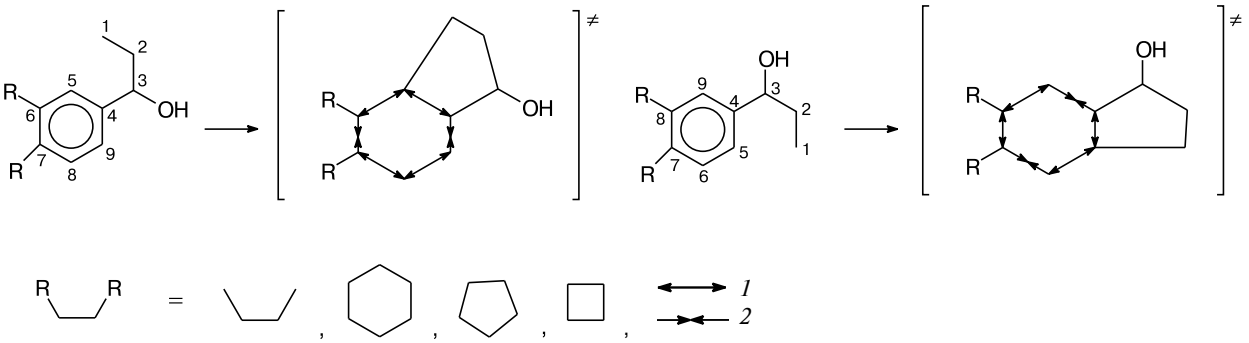

Fig. 2. Direction of changing the bond lengths in the aromatic rings during ketone transformation **17**—**20** → **21**$^{\neq}$—**28**$^{\neq}$: *1*, bond elongation; *2*, bond shortening.

cause on going to the transition state the C(6)—C(7) bond lengths decreases in the case of α-cyclization and the C(7)—C(8) bond length increases in the case of β-cyclization. For compounds **17** and **18** the factor discussed is not principally significant: in the case of compound **18**, the conformational mobility of the six-membered fused fragment compensates the changes in the geometry of the aromatic ring at any direction of cyclization. In the case of intermediates **19** and particularly intermediates **20**, the changes in the geometry of the fused cycles with the retention and even enhancement of the angular strain in them correspond to the transition state of α-cyclization accompanied by a decrease in the C(6)—C(7) bond lengths. On the contrary, in the case of β-cyclization the transition to the transition state is facilitated by the partial elimination of angular strain.

The discussed structural changes can be illustrated for the transitions **20α** → **27**$^{\neq}$ and **20β** → **28**$^{\neq}$, using for the qualitative estimation of the angular strain the change in the total deviation of the bond angles in the four-membered ring from 90°. In the case of α-cyclization this value is +1.386°, whereas for β-cyclization it is −0.831°.

Thus, the experimentally determined ratio of the Nazarov reaction products corresponds to that found by the quantum chemical calculations. For the compounds with the five- and four-membered alicycles, the experimental data coincides well with the computer simulation results. The influence of the saturated fused fragment on the regioselectivity of cyclization cannot be explained only by the electronic effects of alkyl substituents. The reaction is facilitated by distortions in the aromatic ring caused by the fused cycle. The predominant occurrence of the cyclization in the β-position is determined by the partial elimination of the angular strain in the fused cyclic fragments in the corresponding transition state. The presence of the small fused cyclic fragment can be considered as the general structural factor affecting both the reactivity of aromatic compounds and regioselectivity of the process.

Experimental

Calculation procedure. Calculations were performed using the PRIRODA program[10] and PBE functional[11] including the electron density gradient and the extended basis sets of the Gaussian functions. In the present study, the orbital basis sets have the following compression samples: (5s1p)/[3s1p] for the H atom and (5s5p2d)/[3s3p2d] for the C, O, and Cl atoms. The auxiliary basis sets are the uncompressed sets of the Gaussian functions of the sizes (5s1p) for the H atom and (6s3p3d1f) for the C, O, and Cl atoms. Ten electrons of internal shells for the Cl atom and two electrons for the C and O atoms were described using the pseudo-potentials (ECP).[12—14]

The full geometry optimization of all structures described in the work (both the complexes and transition state) was performed without restrictions to the symmetry of the molecule using analytical gradients. The character of the determined stationary points was found on the basis of the analytical calculation of the secondary energy derivatives with respect to coordinates.

The thermodynamic characteristics presented in this work and the vibrational frequencies were calculated in the approximations of harmonic oscillator, rigid rotator, and ideal gas. The vibrational spectrum of all calculated reactants, intermediates, and reaction products contain no imaginary frequency, and the vibrational spectrum of all optimized transition states has one imaginary mode corresponding to the reaction coordinate.

Synthetic procedures. All experiments were carried out in an argon atmosphere. Methylene chloride was purified by distillation over CaH_2. Nitromethane, 3-chloropropionyl chloride, *o*-xylene, tetralin, and indane (ACROS) were used without additional purification. ^{1}H and ^{13}C NMR spectra were recorded on a Varian VXR-400 instrument at 20 °C in $CDCl_3$.

All compounds synthesized in the present work are described, but no NMR data are presented in the literature. In addition, some procedures for the synthesis and isolation were modified and, hence, their description is given in this work along with the NMR spectral data for compounds **1**—**8**.

Synthesis of compounds 1—4 (general procedure). Aluminum trichloride $AlCl_3$ (24 g, 0.18 mol) was added with vigorous stirring to a solution (cooled to 0 °C) of 3-chloropropionyl chloride (19.7 g, 0.155 mol) in CH_2Cl_2 (200 mL). The corresponding arene (0.15 mol) was added dropwise to the resulting suspension for 30 min, maintaining the temperature of the reaction mixture

about 5 °C. After 1 h the cooling was removed, and the mixture was left to stay at ambient temperature. Then the reaction mixture was carefully quenched with a mixture of a saturated solution of HCl (30 mL), cold water (150 mL), and ice (150 g). The organic layer was separated, and the aqueous solution was extracted with chloroform (3×50 mL). The combined organic phases were washed with water, a 5% solution of Na_2CO_3, and again with a minimum water, dried over Na_2SO_4, and concentrated *in vacuo*.

3-Chloro-1-(3,4-dimethylphenyl)propan-1-one (1). The yield was 98% (light gray powder). ^{1}H NMR, δ: 2.33 (br.s, 6 H); 3.42 (t, 2 H, J = 6.8 Hz); 3.92 (t, 2 H, J = 6.8 Hz); 7.23 (d, 1 H, J = 7.7 Hz); 7.69 (d, 1 H, J = 7.7 Hz); 7.74 (s, 1 H).

3-Chloro-1-(5,6,7,8-tetrahydro-2-naphthyl)propan-1-one (2). The yield was 98% (beige powder). ^{1}H NMR, δ: 1.83 (m, 4 H); 2.82 (m, 4 H); 3.42 (t, 2 H, J = 6.8 Hz); 3.91 (t, 2 H, J = 6.8 Hz); 7.16 (d, 1 H, J = 8.4 Hz); 7.69—7.65 (m, 3 H).

3-Chloro-1-(2,3-dihydro-1*H*-inden-5-yl)propan-1-one (3). The yield was 94%. ^{1}H NMR, δ: 2.13 (q, 2 H, J = 7.5 Hz); 2.97 (t, 4 H, J = 7.5 Hz); 3.44 (t, 2 H, J = 6.9 Hz); 3.92 (t, 2 H, J = 6.9 Hz); 7.31 (d, 1 H, J = 7.9 Hz); 7.76 (d, 1 H, J = 7.9 Hz); 7.82 (s, 1 H).

1-(Bicyclo[4.2.0]octa-1,3,5-trien-3-yl)-3-chloropropan-1-one (4) was obtained according to the general procedure using nitromethane as a solvent. The residue after evaporation was recrystallized from hexane. The yield was 63% (pale pink powder). ^{1}H NMR, δ: 3.23 (br.s, 4 H); 3.43 (t, 2 H, J = 6.8 Hz); 3.92 (t, 2 H, J = 6.8 Hz); 7.15 (d, 1 H, J = 8 Hz); 7.65 (s, 1 H); 7.85 (d, 1 H, J = 8 Hz).

Synthesis of compounds 5—8 (general procedure). The corresponding 1-aryl-3-chloropropan-1-one (0.1 mol) was added in small portions with vigorous stirring to concentrated H_2SO_4 (150 mL) heated to 80 °C. The stirring was continued at 85—90 °C until the end of gas evolution (1 h), monitoring by TLC in chloroform. Then the reaction mixture was cooled to 20 °C, carefully poured into water (150 mL) with ice (150 g), and extracted with chloroform (3×50 mL). The combined extracts were dried over Na_2SO_4 and concentrated by evaporation. The ratio of the cyclization products was determined by the analysis of the ^{1}H NMR spectra.

4,5-Dimethylindan-1-one (5) and 5,6-dimethylindan-1-one (6). The overall yield was 80%, white powder. ^{1}H NMR spectrum of compound **5**, δ: 2.25 (s, 3 H); 2.37 (s, 3 H); 2.67 (t, 2 H, J = 5.8 Hz); 3.00 (t, 2 H, J = 5.8 Hz); 7.17 (d, 1 H, J = 7.7 Hz); 7.51 (1 H). ^{1}H NMR of compound **6**, δ: 2.30 (s, 3 H); 2.34 (s, 3 H); 2.64 (t, 2 H, J = 5.9 Hz); 3.04 (t, 2 H, J = 5.9 Hz); 7.24 (s, 1 H); 7.50 (s, 1 H).

1,2,6,7,8,9-Hexahydro-3*H*-cyclopenta[*a*]naphthalen-3-one (7) and **2,3,5,6,7,8-hexahydro-1*H*-cyclopenta[*b*]naphthalen-1-one (8).** The overall yield was 53%, white powder. ^{1}H NMR spectrum of compound **7**, δ: 1.80—1.90 (m, 4 H); 2.62—2.71 (m, 4 H); 2.84 (t, 2 H, J = 5.6 Hz); 2.93 (t, 2 H, J = 5.6 Hz); 7.08 (d, 1 H, J = 7.9 Hz); 7.48 (d, 1 H, J = 7.9 Hz). ^{1}H NMR of compound **8**, δ: 1.80—1.90 (m, 4 H); 2.62—2.71 (m, 4 H); 2.83 (t, 2 H, J = 5.7 Hz); 3.04 (t, 2 H, J = 5.7 Hz); 7.16 (s, 1 H); 7.45 (s, 1 H).

1,6,7,8-Tetrahydro-*asymm*-(2*H*)-indacen-3-one (9) and **3,5,6,7-tetrahydro-*symm*-(2*H*)-indacen-1-one (10).** The overall yield was 75%, white powder. The ratio **9** : **10** was 1 : 4.5. ^{1}H NMR spectrum of compound **9**, δ: 2.20 (q, 2 H, J = 7.3 Hz); 2.68—2.71 (2 H); 2.90—3.02 (6 H); 7.24 (d, 1 H, J = 7.7 Hz); 7.58 (d, 1 H). ^{1}H NMR spectrum of compound **10**, δ: 2.13 (q, 2 H, J = 7.3 Hz); 2.68 (t, 2 H, J = 7.3 Hz); 2.92 (t, 2 H, J = 7.3 Hz); 2.95 (t, 2 H, J = 5.8 Hz); 3.07 (t, 2 H, J = 5.8 Hz); 7.29 (s, 1 H); 7.57 (s, 1 H).

1,2,5,6-Tetrahydro-4*H*-cyclobuta[*f*]inden-4-one (12). The yield was 45%, pale pink powder. ^{1}H NMR, δ: 2.65 (t, 2 H, J = 5.8 Hz); 3.10 (t, 2 H, J = 5.8 Hz); 3.19 (br.s, 4 H); 7.14 (s, 1 H); 7.41 (s, 1 H).

References

1. N. B. Ivchenko, P. V. Ivchenko, I. E. Nifant´ev, *Zh. Org. Khim.*, 1999, **35**, 641 [*Russ. J. Org. Chem.* (*Engl. Transl.*), 1999, **35**].
2. W. Kaminsky, O. Rabe, A.-M. Schauwienold, G. U. Schupfner, J. Hanss, J. Kopf, *J. Organomet. Chem.*, 1995, **497**, 181.
3. U. Dietrich, M. Hackmann, B. Rieger, M. Klinga, M. Leskela, *J. Am. Chem. Soc.*, 1999, **121**, 4348.
4. L. Resconi, S. Guidotti, I. Camurati, R. Frabetti, F. Focante, I. E. Nifant'ev, I. P. Laishevtsev, *Macromol. Chem.*, 2005, **206**, 1405.
5. R. T. Hart, R. F. Hart, *J. Am. Chem. Soc.*, 1950, **72**, 3286.
6. K. R. Koltunov, S. Walspurger, J. Sommer, *Tetrahedron Lett.*, 2005, **46**, 8391.
7. W. Bartmann, E. Konz, W. Rueger, *J. Heterocycl. Chem.*, 1987, **24**, 677.
8. L. Horner, K. Muth, H.-G. Schmelzer, *Chem. Ber.*, 1959, **92**, 2953.
9. D. V. Avila, A. G. Davies, E. R. Li, K. M. Ng, *J. Chem. Soc., Perkin Trans. 2*, 1993, 355.
10. D. N. Laikov, *Chem. Phys. Lett.*, 1997, **281**, 151.
11. J. P. Perdew, K. Burke, M. Ernzerhof, *Phys. Rev. Lett.*, 1996, **77**, 3865.
12. W. J. Stevens, H. Basch, M. Krauss, *J. Chem. Phys.*, 1984, **81**, 6026.
13. W. J. Stevens, M. Krauss, H. Basch, P.G.Jasien, *Can. J. Chem.*, 1992, **70**, 612.
14. T. R. Cundari, W. J. Stevens, *J. Chem. Phys.*, 1993, **98**, 5555.

Received July 15, 2008;
in revised form January 12, 2009